to that of **1**. Rather effective binding of sugars by octadecyl alcohol (**2**) monolayer is consistent with this mechanism.

The high sensitivity of the electrode response (at 10^{-5} M sugars) is surprising. The extraction experiment of **1**-CCl_4-water system required much higher guest concentrations, typically 3-5 M for sugars.[12] These high concentrations were not necessary in the present work. The much enhanced sugar binding at the interface may be produced by either or both of the following factors. First, host molecules are aligned at the interface in a high density. This is expected to shift the equilibrium in favor of complex formation and to help sugar binding entropically. The advantage of multisite guest molecules like poly(vinylpyrrolidone) is obvious. Secondly, the structure of water at the interface is different from that of bulk water.[28] Host compound **1** in the bulk phase is strongly hydrogen-bonded to water, forming a stable tetrahydrate. The pattern and strength of hydrogen bonding with water may change extensively when this compound is in contact with the interfacial water.[12] The water of hydration may become more exchangeable relative to that in the bulk. The anisotropic alignment of the host functional group could also modify the pattern of hydration, enhancing sugar binding at low concentrations.

(28) Israelachivili, J. N. *Intermolecular and Surface Forces*; Academic Press: London, 1985.

Previous examples of well-defined guest monolayers are limited, especially with regard to organic guest molecules. Inclusion of azobenzene derivatives in cyclodextrin monolayers has been monitored by visible absorption spectroscopy and by circular dichroism.[5b] In this case, the host-guest monolayers were formed by spreading organic solutions of host and guest molecules (complexes) over the aqueous subphase; thus the host-guest interaction is not induced at the interface. Specific interactions of nucleolipid monolayers with water-soluble organic molecules have been studied only by the π-A isotherm data.[4] The present investigation represents, to the best of our knowledge, the first example of direct observation of guest binding to a monolayer.

Conclusions

It is demonstrated for the first time that molecular recognition is effectively accomplished by a hydrogen-bonding host monolayer that is exposed to aqueous subphases. The unexpected effectiveness is attributable to the high density of host molecules and peculiar properties of water at the interface. The mode of sugar binding is apparently different between the bulk phase and the interface. These features may be related to unique biological processes occurring at the cell membrane surface. An important implication of the present result is that novel chemical sensors can be designed on the basis of two-dimensional alignment of specifically interacting functional groups.

Formation of Organic Thin Films by Electrolysis of Surfactants with the Ferrocenyl Moiety

Tetsuo Saji,* Katsuyoshi Hoshino, Yoshiyuki Ishii, and Masayuki Goto

Contribution from the Department of Chemical Engineering, Tokyo Institute of Technology, Ohokayama, Meguro-ku, Tokyo 152, Japan. *Received July 6, 1990*

Abstract: The formation of organic thin films by controlled-potential electrolysis (oxidation) of an aqueous solution containing surfactants with a ferrocenyl moiety and an organic compound incorporated in micelles or in a dispersed organic pigment with use of the surfactants is examined. Opaque films of five azo dyes, vinylcarbazole, cetyl alcohol, dioctadecyldimethylammonium chloride, and 4,4′-didodecylviologen are formed through the former mechanism. Transparent films of phthalocyanine compounds (MPc (M = H_2, Cu)), four halogen derivatives of CuPc, three perylene derivatives, and two quinones are formed through the latter mechanism. The scanning electron micrograph studies show that crystal size of the film increases with electrolysis time in the case of the former mechanism and is the same for the added particles in the case of the latter mechanism. The adsorption isotherm of the surfactant on the pigment particle surface shows that they form monolayers at saturation and their desorption starts at slightly above the critical micelle concentration (cmc). These results suggest that the films formed through the former and the latter mechanisms are prepared by disruption of micelles and desorption of surfactant from the pigment surface, respectively.

Introduction

Although electrochemistry of organic compounds solubilized in micellar solutions has been extensively studied by several researchers,[1] no electrochemistry of micelles formed by redox-active surfactants has been reported. Recently, we demonstrated that a micelle formed by surfactants with the ferrocenyl moiety can be broken up into monomers when the surfactants are oxidized chemically or electrochemically.[2,3] Reversibility of such control

Scheme I

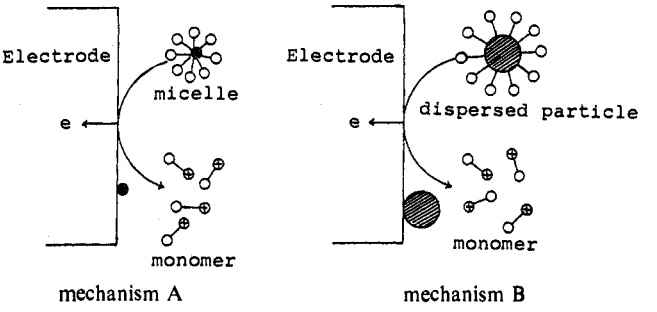

of the formation-disruption of a micelle was also demonstrated by a spectroscopic observation that a dye is solubilized or released accordingly as the micelles are formed or broken up. This procedure was extended to preparation of organic thin films.[4] This

(1) (a) Hayano, S.; Shinozuka, N. *Bull. Chem. Soc. Jpn.* **1969**, *42*, 1469-1472. (b) Yeh, P.; Kuwana, T. *J. Electrochem. Soc.* **1976**, *123*, 1334-1339. (c) Ohsawa, Y.; Aoyagui, S. *J. Electroanal. Chem.* **1980**, *114*, 235-246. (d) McIntire, G. L.; Chiappardi, D. M.; Casselberry, R. L.; Blount, H. N. *J. Phys. Chem.* **1982**, *86*, 2632-2640. (e) Rusling, J. F.; Kamau, G. N. *J. Electroanal. Chem.* **1985**, *187*, 355-359.

(2) Saji, T.; Hoshino, K.; Aoyagui, S. *J. Am. Chem. Soc.* **1985**, *107*, 6865-6868.

(3) Saji, T.; Hoshino, K.; Aoyagui, S. *J. Chem. Soc., Chem. Commun.* **1985**, 865-866.

0002-7863/91/1513-450$02.50/0

Chart I

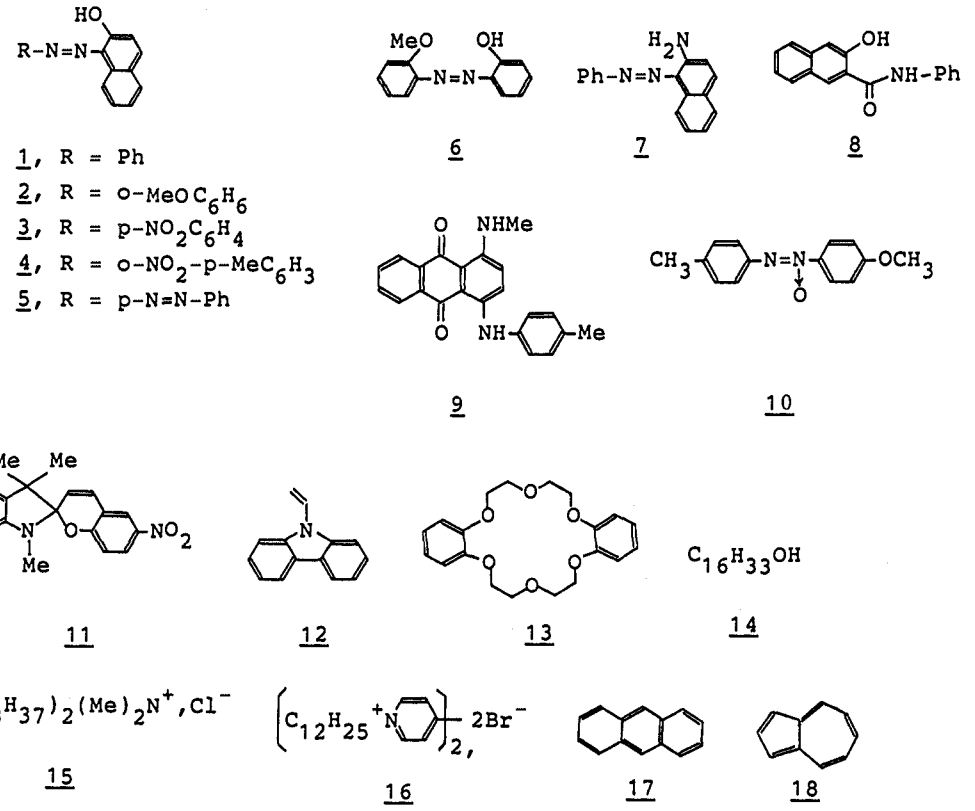

novel film-formation method (micelle-disruption method, MD method) is based on the controlled release of a micelle-solubilized substance onto an electrode. The micelles formed by the surfactants are broken up into monomers when the surfactants are electrochemically oxidized. A solubilizate is then released from the micelles and deposited onto the electrode (Scheme I, mechanism A). Organic films of 1-(phenylazo)-2-naphthol, 1,1′-didodecyl-4,4′-bipyridinium dibromide, and some polymers have been prepared.[4-6] In addition, we reported the preparation of thin films of phthalocyanine and of its copper complexes by electrolysis of nonionic surfactants with the ferrocenyl moiety.[7] Scanning electron micrographs of these pigment powders and their films suggest that these compounds are dispersed by the surfactants and not incorporated in the micelles. The particles of these compounds are released when the adsorbed surfactants on particles are electrochemically oxidized and deposited on the electrode (Scheme I, mechanism B). In this paper, we describe the preparation and characterization of the organic thin films and discuss the difference between these two mechanisms.

Experimental Section

Materials. Compounds **1–18** were purchased commercially and used as received except for **16**. Compound **16** was prepared by the literature method[8] (Chart I). Compounds **19** and **25** were purchased from Tokyo Kasei Kogyo Co. Ltd., and **22** was purchased from Kanto Chemical Co., Inc. Compounds in Table II, except **19** and **25**, were donated by the following companies: **20**, **21**, and **24**, Dainichiseika Color & Chemicals Mfg. Co. Ltd.; **23**, Toyo Inki Co. Ltd.; **26–28** and **33**, BASF Japan Ltd.; **29** and **31**, Bayer Japan Ltd.; **32**, Ciba-Geigy; **34** and **35**, Hoechst Japan Ltd. (Chart II). Brij 35 (poly(oxyethylene) (23)) was purchased from Wako Pure Chemicals. Compounds **28–35** were washed with distilled water in order to remove unidentified impurities, which influence cohesive forces between these compounds and the electrode.

Preparation of (11-Bromoundecanoyl)ferrocene. A solution of 11-bromoundecanoic acid (25 g, 94 mmol) in 20 mL of $SOCl_2$ was stirred for 1 day. The solution was evaporated to give crude 11-bromoundecanoyl chloride.[9] A solution of the crude compound in 40 mL of CH_2Cl_2 was added dropwise to 16.7 g (90 mmol) of ferrocene and 12.4 g (94 mmol) of $AlCl_3$ in 100 mL of CH_2Cl_2 over 1 h under N_2. After it was stirred overnight, the solution was poured into ice–water saturated with NaCl. The organic layer was separated, washed with water saturated with NaCl, dried with $MgSO_4$, and evaporated. The residue was extracted with hot methanol, evaporated, and passed through a column of silica gel (Wakogel G, benzene) to give a reddish solid (26 g, 65%) of (11-bromoundecanoyl)ferrocene. Recrystallization from methanol gave yellow crystals: UV–vis (ethanol) 337 nm (ϵ 1200), 458 (454); mp 55.5–56.5 °C; ^{1}NMR ($CDCl_3$) δ 4.7 (2 H, $H_{ferrocene}$), 4.4 (2 H, $H_{ferrocene}$), 4.1 (5 H, $H_{ferrocene}$), 3.3 (2 H, $-CH_2Br$), 2.6 (2 H, $-COCH_2-$), 1.8 (2 H, $-CH_2CH_2Br$), 1.6 (2 H, $-COCH_2CH_2-$), 1.3 (12 H, $-(CH_2)_2CH_2-(CH_2)_2-$). Anal. Calcd for $C_{21}H_{29}OBrFe$: C, 58.22; H, 6.74; N, 0.00. Found: C, 58.06; H, 6.93; N, 0.00.

Preparation of (11-Bromoundecyl)ferrocene (BUFC). A solution of 47% HBr (52.8 mL) in 120 mL of ethanol was added to a stirred mixture of (11-bromoundecanoyl)ferrocene (12 g, 28 mmol), 400 mL of ethanol, and amalgamated zinc, which was prepared with 53 g of Zn, 7.1 g of $HgBr_2$, and a small amount of dilute HBr, over 30 min under N_2 at 70–75 °C. After the mixture was refluxed for 1 h, the solution was evaporated and the residue extracted with ether, dried with $MgSO_4$, and evaporated to dryness. The residue was passed through silica gel (hexane, second yellow band) to give yellow crystals (3.1 g, 26%) of BUFC: UV–vis (ethanol) 326 nm (ϵ 60), 437 (98); mp 38.5–39.5 °C; ^{1}NMR ($CDCl_3$) δ 4.0–4.1 (9 H, $H_{ferrocene}$), 3.4 (2 H, $-CH_2CH_2Br-$), 2.2–2.3 (2 H, ferrocene–CH_2-), 1.8 (2 H, $-CH_2CH_2Br$), 1.3 (16 H, $-CH_2CH_2CH_2-$). Anal. Calcd for $C_{21}H_{31}BrFe$: C, 60.16; H, 7.45; N, 0.00. Found: C, 60.34; H, 7.44; N, 0.00.

Preparation of (11-Ferrocenylundecyl)trimethylammonium Bromide (FTMA). To 2.48 g (5.9 mmol) of BUFC was added under N_2 a solution of trimethylamine (0.4 M) in 15 mL of ethanol. The mixture was stirred at 60 °C for 2 days, evaporated, washed with hexane, and recrystallized from acetone–hexane. The yellow solid was dried under vacuum to give a yellow solid (1.6 g, 57%) of FTMA: UV–vis (ethanol) 326 nm (ϵ 60), 438 (96); ^{1}NMR ($CDCl_3$) δ 4.0–4.1 (9 H, $H_{ferrocene}$), 3.6 (2 H,

(4) Hoshino, K.; Saji, T. *J. Am. Chem. Soc.* **1987**, *109*, 5881–5883.
(5) Hoshino, K.; Saji, T. *Chem. Lett.* **1987**, 1439–1442.
(6) Hoshino, K.; Goto, M.; Saji, T. *Chem. Lett.* **1987**, 547–550.
(7) (a) Saji, T. *Chem. Lett.* **1988**, 693–696; (b) Saji, T.; Ishil, Y. *J. Electrochem. Soc.* **1989**, *136*, 2953–2956.
(8) Pileni, M. P.; Braun, A. M.; Grätzel, M. *Photochem. Photobiol.* **1980**, *31*, 423–427.
(9) McKay, A. F.; Garmaise, D. L.; Baker, H. A.; Hawkins, L. R.; Falta, V.; Gaudry, R.; Paris, G. Y. *J. Med. Chem.* **1963**, *6*, 587–595; *Chem. Abstr.* **1963**, *59*, 12668g.

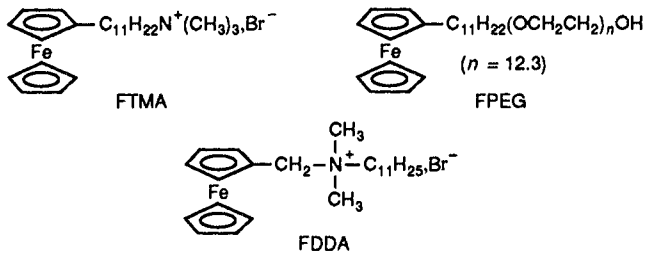

$-CH_2N^+(CH_3)_3$), 3.4 (9 H, $-N^+(CH_3)_3$), 2.3 (2 H, ferrocene–CH_2–), 1.8 (2 H, $-CH_2CH_2N^+(CH_3)_3$), 1.3 (16 H, $-CH_2CH_2CH_2-$). Anal. C, H, N.

Preparation of α-(11-Ferrocenylundecyl)-ω-hydroxypoly(oxyethylene) (12.3) (FPEG). To 12 g of poly(oxyethylene) (average molecular weight 600) were added under N_2 small pieces of sodium metal (80 mg, 3.6 mmol). The mixture was stirred at 70–100 °C for 4 h with an occasional scratching of the sodium metal surface with a spatula, and 1.0 g (2.4 mmol) of BUFC was added. The mixture was maintained at 110 °C for 10 h. After the mixture was cooled to room temperature, the mixture was extracted with 50% butanol–water. The organic layer was extracted twice with water saturated with NaCl, dried over magnesium sulfate, evaporated, and passed through silica gel twice (benzene:ethanol = 5:1) to give a yellow oil (0.93 g, 39%) of FPEG: UV–vis (ethanol) 326 nm (ε 64), 438 (100); ^1H NMR ($CDCl_3$) δ 4.0–4.1 (9 H, $H_{ferrocene}$), 3.5–3.7 (50.7 H, $-OCH_2CH_2O-$, $-(CH_2)_2CH_2O-$), 2.2–2.3 (2 H, ferrocene–CH_2–), 1.6 (2 H, $-CH_2CH_2CH_2O-$), 1.3 (6 H, $-CH_2CH_2CH_2-$). Anal. Calcd for $C_{45.6}H_{81.2}O_{13.3}Fe$: C, 60.98; H, 9.11; N, 0.00. Found: C, 60.60; H, 9.50; N, 0.00.

Preparation of (ferrocenylmethyl)dodecyldimethylammonium bromide (FDDA) has been described in our previous paper.[2]

FTMA and FPEG in an aqueous solution were stable for a few months under dark, and FDDA was slowly decomposed.

Electrochemical Cell. Controlled-potential electrolysis and cyclic voltammetry were carried out with a three-electrode cell. An indium tin oxide electrode (ITO) and a saturated calomel electrode (SCE) were used as a working and a reference electrode, respectively. The ITO was obtained from Matsuzaki Shinku Co. (10 Ω/square). The auxiliary electrode was a platinum plate. The dimensions of the ITO were 20 mm × 10 mm × 1.1 mm, and the zone area in contact with solution was 10 mm × 10 mm. This ITO was cleaned by sonication in distilled water for 5 min followed by subsequent sonication with acetone, chloroform, and distilled water for 5 min.

Controlled-potential electrolysis and cyclic voltammetry were performed with a Model NPGFZ-2501-A potentiogalvanostat (Nikko Keisoku Co.). The amount of electricity passed through an electrode was measured with a Model HF-201 coulomb per ampere hour meter (Hokuto Denko Co.). Electrochemical measurements were done at 25 °C under N_2.

Absorption spectra were recorded on a Hitachi UV 220 spectrophotometer. Scanning electron micrographs (SEM) and transmission electron micrographs (TEM) were obtained with Nippon Denshi JSM-T220 and JEM-100 CX instruments, respectively. Organic films were coated with 100 Å of Au to minimize problems from surface charging. Film thicknesses were measured with a Model BM-2 multiple-beam interferometer (Mizojiri Kogaku Co.)[10] or directly with the SEM for the cross sections of films.

Film Formation. The solutions of organic compounds in Table I were prepared by adding an excess amount of the organic compound, used as a film-forming material, to an aqueous micellar solution containing the surfactant and supporting electrolyte. The concentration of the surfactant was 2.0 mM. The supporting electrolyte was 0.2 M Li_2SO_4 (for FTMA) or 0.1 M LiBr (for FPEG). The suspension was sonicated for 5–10 min and then stirred for 3–7 days at 25 °C to attain solubilization equilibrium. Undissolved organic compounds in Table I were removed by centrifugation (2000 rpm, 1 h). The concentration of the organic compound with a chromophore incorporated in the micelles in Table I was determined by their absorption spectra: The molar absorption coefficient of the compound was determined in an aqueous micellar solution of 0.1 M dodecyltrimethylammonium bromide or in ethanol. The compounds without a chromophore were solubilized by adding their acetone or ethanol–acetone solutions to the aqueous micellar solutions. The organic solvent, i.e., acetone and/or ethanol, was removed by bubbling N_2 through the solution. The concentrations of these compounds were calculated from the amount of the added acetone solution.

(10) Tolansky, S. *Interferometry of Surfaces and Films*; Oxford University Press: London, 1948.

Table I. Results of Film-Formation Studies of Organic Compounds Incorporated in the Micelles in 2 mM Surfactant–0.2 M Li_2SO_4 (0.1 M LiBr for FPEG) Aqueous Solution

cmpnd	surfactant	C_{sol}, μM	electrol time, min	Q, mC cm^{-2}	appearance[a]
1	FTMA	39	70	74	orange
2	FPEG	90	210	62	orange
3	FTMA	5	830	150	red
4	FPEG	61	970	340	no film
5	FTMA	36	790	290	no film
6	FTMA	27	1100	670	red
7	FTMA	410	860	64	yellow
8	FTMA	36	1530	770	white
9	FTMA	10	750	990	no film
10	FPEG	220	170	630	no film
11	FTMA	27	200	95	white
12	FTMA	420	50	15	white
13	FPEG	100	870	740	no film
14	FTMA	180	140	62	white
15	FTMA	63	840	67	white
16[b,c]	FTMA	800	40	100	white
17	FPEG	22	190	150	no film
18	FPEG	660	940	730	no film

[a] All of the films in this table are opaque. [b] Obtained with glassy-carbon electrode, others with indium tin oxide electrode. [c] Reference 5.

Table II. Results of Film-Formation Studies of Organic Compounds Dispersed in 2 mM FPEG–0.1 M LiBr Aqueous Solution

cmpnd	particle size, μm	C_{added}, mM	C_{disp}, mM	electrol time, min	Q, mC cm^{-2}	appearance[a]
19[b]	0.1–0.2	10	3	30	16	greenish blue
20[c]	0.1–0.2	10	7	30	10	blue
21[c]	0.1–0.2	10	4	30	10	blue
22[c]	2–5	10	1	60		no film
23[c]	0.05–0.1	10	4	20	7	blue
24	0.05–0.1	10	5	20	12	blue
25	0.05–0.1	20	11	20	6	bluish green
26	0.05–0.1	10	8	20	10	green
27	0.05–0.1	10	3	20	7	green
28	0.2–0.4	20	18	40	6	red
29	0.03–0.04	10	9	40	4	red
30	0.1–0.4	20	18	40	19	red
31	0.05–0.1	15	8	90	13	red
32	0.02–0.04	15	11	80	29	red
33	0.2–0.3	12	8	30	3	red
34	0.1–0.2	10	*d*	30		no film
35	0.1–0.2	10	*d*	30		no film

[a] All of the films in this table are transparent. [b] Reference 7a. [c] Reference 7b. [d] Sediment.

Table III. Half-Wave Potential ($E_{1/2}$), Critical Micelle Concentration (cmc), and Solubilization of **1** in 2 mM Surfactant with a Ferrocenyl Moiety Aqueous Solution Containing 0.2 M Li_2SO_4 ($\mathbf{1}_{sat}$)

surfactant	$E_{1/2}$ vs SCE, V	cmc, mM	$\mathbf{1}_{sat}$, μM
FDDA	+0.43	5×10^{-1}	29
FTMA	+0.15	7×10^{-2}	39
FPEG	+0.28	8×10^{-3}	80

The solutions of organic compounds in Table II were prepared in the following manner: An aqueous solution containing 2.0 mM FPEG, 0.1 M LiBr, and known amounts of the organic compound was sonicated for 10 min and stirred for 3 days. The amount of compound dispersed in this solution in Table II was estimated by weighing the residue that was obtained after evaporation of the solution and drying over phosphorus pentoxide in a desiccator for 1 week. The amount of **21** deposited on the ITO electrode in the film-growth experiment was estimated by the absorption of the aqueous solution that was obtained by redispersing the film into an aqueous solution of 3 mM Brij 35, where the absorptivity of 24 200 M^{-1} cm^{-1} at 714 nm for **21** was used. Film formation was undertaken by the controlled-potential electrolysis of the supernatant of these solutions. The solutions were deaerated by bubbling N_2 for at least 20 min. N_2 was also passed over the solution during the electrolysis. The solution was stirred with a magnetic stir bar 1 cm long at 60–80 rpm in

Chart II

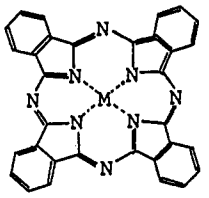

MPc

19, M = H_2
20, M = Cu; α-form
21 and 22, M = Cu; β-form
23, M = Cu; ε-form

$CuPcBr_xCl_y$

24, x = 0; y = 1
25, x = 0; y = ~16
26, x = ~6; y = ~10
27, x = ~8; y = ~8

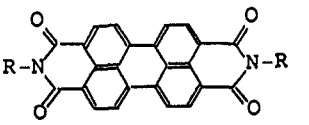

28 and 29, R = EtO-C_6H_4
30, R = p-Ph-N=N-C_6H_4
31, R = Me

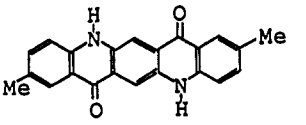

34

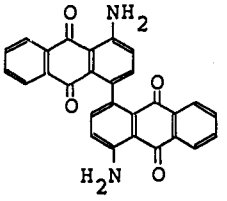

32

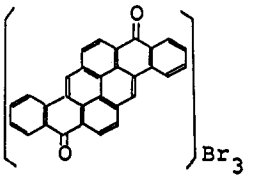

33

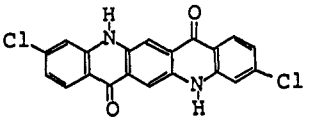

35

the case of mechanism A and was not stirred in the case of mechanism B in Scheme I. The potential of the ITO was maintained at +0.30 V vs SCE for the FTMA solutions and at +0.50 V for the FPEG solution by considering the half-wave potentials of these surfactants (Table III). The obtained films were washed with distilled water just after electrolysis or dried under air for 1 day and then washed with distilled water when adhesion of the film was weak.

Adsorption Isotherm. To 12 mL of FPEG solution was added 68.9 mg of **21** (10 mM). This solution was sonicated for 15 min, stirred for 3 days, and centrifuged (Hitachi SCP 70H) at 40 000 rpm (110 000*g*) for 40 min. The surfactant concentration in the supernatant (C_{eq}) was determined by the following colorimetric technique:[11] After the supernatant was diluted to an appropriate concentration, 5 mL of this solution was mixed with 1 mL of 1.0 mM KI and 0.5 mM I_2 aqueous solution and then the absorbances at 460, 480, and 500 nm were measured. The concentration was determined with use of the calibration curves in the surfactant concentration range 0–20 μM. The amount of the adsorbed surfactants (Γ) was estimated with the relationship $\Gamma = (C_0 - C_{eq})/S$, where C_0 and S are the initial concentration of surfactant and the surface area of the pigment powders, respectively. The geometric area of **21** powders (80 $m^2\ g^{-1}$) was estimated from the SEM of **21** powders.

Results and Discussion

Properties of Surfactants. Table III shows the physicochemical properties of FDDA, FTMA, and FPEG in 0.2 M Li_2SO_4 aqueous solution. The cyclic voltammograms of these solutions showed a reversible one-electron step. Half-wave potentials ($E_{1/2}$) of the surfactants were obtained by a midpoint potential between the anodic peak potential and the cathodic one in the cyclic voltammetry at a platinum disk electrode.[12] The values of critical micelle concentrations (cmc) of these surfactants were determined by the usual dye solubilization method with **1**.[13] The cmc value of FPEG (8 μM) was nearly equal to that obtained by the surface tension method (10 μM). The cmc value was in the order of FPEG < FTMA < FDDA (Table I). The small cmc of FPEG may result from the absence of any dissociable groups.[14] In the film-forming experiments, the concentration of the surfactant was 2.0 mM, so the concentration of its monomer may be negligible compared with the concentration of the surfactant except for the case of FDDA. Solubilization power of the surfactants is represented by the saturated concentration of **1** in 2.0 mM of the surfactant solution

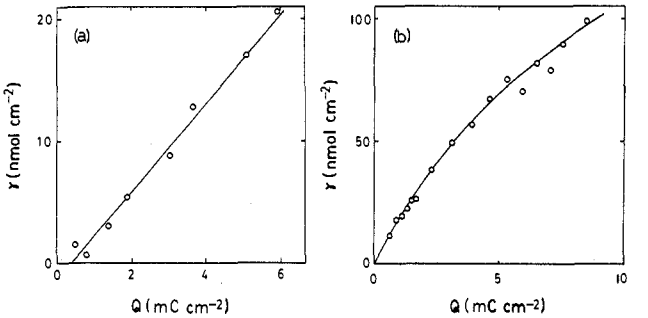

Figure 1. Amount of film (γ) versus that of electricity passed through the electrode (Q): (a) **16**; (b) **21**.

containing 0.2 M Li_2SO_4, $\mathbf{1}_{sat}$ (Table III). This dye was sparingly soluble in an 0.2 M Li_2SO_4 solution devoid of any surfactant. The solubilization power of the surfactants was in the increasing order of FDDA < FTMA < FPEG, opposite to the order of cmc.

Film Formation through Mechanism A, Scheme I. Table I lists the organic compounds that may be solubilized by incorporation in the micelles. It is generally believed that polar compounds such as **1–11** are incorporated by adsorption in the micelles, partially miscible polar compounds such as **14–16** penetrate into the palisade layer of the micelles, and nonpolar compounds such as **17** and **18** are incorporated into the hydrocarbon interior of the micelles.[15]

The results of film formations are listed in the last column in Table I. Films of 11 compounds were formed. All of these films appeared opaque. The films of **7**, **12**, **14**, and **16** grew thicker than 1 μm during ca. 1 h of electrolysis. The values of C_{sat} of these compounds are much higher than those of others. On the other hand, the films of other compounds did not grow more than 0.1 μm during ca. 1 h of electrolysis. The films of **3**, **4**, and **8** were thin even after 14–18 h of electrolysis. These experimental facts suggest that the growth of a film depends on the value of C_{sat}. Figure 1a shows a plot of the amount of **16** deposited on the carbon electrode (γ) versus that of electricity passed through the electrode (Q) without stirring the solution. This linear relationship and the above results may be explained by the dependence of the growth of a film on the amount of the compound released

(11) Baleux, B. *C. R. Acad. Sci., Ser. B.* **1972**, *72*, 1617.
(12) Bard, A. J.; Faulkner, L. R. *Electrochemical Methods*; Wiley: New York, 1980.
(13) For example, see: Tokiwa, F. *J. Phys. Chem.* **1968**, *72*, 1214–1217.
(14) Fendler, J. H.; Fendler, E. J. *Catalysis in Micellar and Macromolecular Systems*; Academic Press: New York, 1975; p 22.
(15) Shinoda, K.; Nakagawa, T.; Tamamushi, B.; Isemura, T. *Colloidal Surfactants*; Academic Press: New York, 1963; pp 139–141.

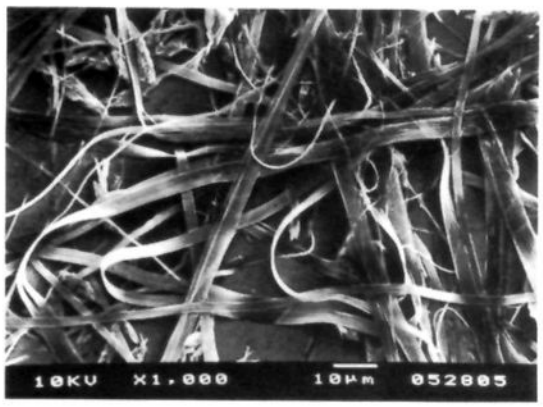

Figure 2. Scanning electron micrograph of surface of the film prepared by the electrolysis of an aqueous solution containing 0.41 mM **7**, 2.0 mM FTMA, and 0.2 M Li_2SO_4 at the electrode for 12 h and 30 min.

from micelles by electrolysis. This amount of the compound is proportional to the number of the molecules solubilized in one micelle (C_{sat}) and that of micelles destroyed by electrolysis. Approximately 70% of **16** released from the micelles by the electrolysis was deposited on the electrode. This percentage is based on the amount of electricity and the number of moles of **16** deposited on the electrode. This value was 51% for the case of **1**.[4] The cyclic voltammogram of the solution of **16** after 30 min of electrolysis showed that the peak current for the surfactant oxidation decreased to only 70% of that without the electrolysis. This result together with those of the SEM images of the films suggests that the electrolysis proceeds through the small space in the film on the electrode.[5] As a typical demonstration of a thick film, the SEM image of **7** is shown in Figure 2. A continuous lacelike network was observed in the image. The films of **8**, **11**, **14**, and **15** consisted of coarse grains.

The films of **4**, **5**, **9**, **10**, **13**, **17**, and **18** were not formed even after more than 10 h of electrolysis. Compounds such as **10**, **13**, and **17** precipitated during electrolysis, suggesting that cohesive forces between these compounds and the ITO electrode are so weak that they were not held on the ITO electrode.

On the basis of these results, we speculate the mechanism of the film formation through mechanism A of Scheme I as follows:

(i) The surfactant monomer is oxidized to its cation. The concentration of this monomer decreases to less than the cmc.

(ii) The micelle-solubilizing organic molecules break up into the monomers in order to satisfy the equilibrium between the micelle and the monomer.

(iii) Organic molecules are released from the micelle as a result of the disappearance of the micelle and deposit on the electrode.

(iv) After the electrode is covered with the organic molecules, the monomers diffuse in the film owing to the existence of small space in the film and are oxidized at the electrode. The decrease of the concentration of the monomer in the vicinity of the film leads the micelle to break up into the monomers so that the film continues to grow.

Film Formation through Mechanism B, Scheme I. Table II lists the organic compounds that may be dispersed by 2.0 mM surfactant (FPEG) in 0.1 M LiBr aqueous solution. The dispersion of these compounds is based on the following reasons: First, the concentrations of these compounds in Table II, C_{disp}, are much larger than those in Table I. Second, the concentration depends on the size of the particles (**21**, **22**, **28**, and **29**). Generally, the smaller particles are advantageous for their dispersion due to their slow sedimentation. Third, the SEM of the particles obtained by evaporation of **21** solution showed that size and crystal form of these particles agree with that of the added particles.

The results of film formations are listed in the last column in Table II. All of the films prepared through mechanism B of Scheme I appeared transparent in contrast to the films obtained through mechanism A and became more than 1 μm in thickness after ca. 30 min of electrolysis owing to their higher C_{disp} values in Table II than those in Table I. In order to prepare thick films of **25**, **28**, **31**, and **32**, addition of a larger amount of these compounds was necessary. The concentration of free FPEG not adsorbed on the particles may be higher in these cases. This free FPEG may form micelles owing to its small cmc value (Table III). These micelles may disturb the release of particles when the FPEG adsorbed on the particles is oxidized. The failure of film formations of **22**, **34**, and **35** is ascribable to the low dispersibility of these compounds. The dispersed particles of **34** and **35** were precipitated within 1 day in spite of their small particle size. The aggregation forces among these particles may be stronger than those of other organic compounds in Table II.

The SEM show these films to be composed of particles (Figure 2 in ref 7a and Figure 3). The size and crystal form of the particles in these films were the same as those of the added powders in the surfactant solutions and did not change after 15 min, 1 h, or 10 h of electrolysis (e.g., **19** and **21**). The transparency of these films is ascribable to these small particles. Light scattering is negligible when the size of the particle is less than the wavelength of visible light. The SEMs of the cross sections of **30** and **32** films (Figure 3b,d) show that these are of uniform thickness and the film thicknesses are approximately 1 μm.

After 30 min of electrolysis and the electrode was covered with the compounds, an oxidation current still flowed through the electrode and these films continued to grow through mechanism B of Scheme I. The thicknesses of **20**, **21**, and **23** increased to more than 10 μm during overnight electrolysis. This may be explained by the fact that the surfactant can penetrate into the film, owing to the existence of small space in the film, and eventually reaches the electrode surface. The cyclic voltammogram of the solution of **21** after 30 min of controlled-potential electrolysis at the electrode showed that the peak current for surfactant oxidation decreased to only 60% of that without the electrolysis.

A plot of the amount of **21** deposited on the electrode versus Q does not show a good linear relationship (Figure 1b) in contrast to that of **16** obtained through mechanism A of Scheme I (Figure 1a). This is ascribable to the difference in the film-forming process between these two mechanisms. Most of the current passed through the electrode in mechanism A contributes to film formation. On the other hand, the current in mechanism B partially contributes to film formation, since the free surfactant does not participate in dispersing the pigment. The deposition of pigment occurs by the desorption of the surfactant of the surface coverage of the pigment. The concentration of free surfactant is 1.1 mM (55%) in this experiment. The ratio of free surfactant may change with time in the course of electrolysis, owing to the difference in the diffusion coefficient between the free and adsorbed surfactants.

Adsorption Isotherm of FPEG on the Pigment Particles. Measurements of the adsorbed FPEG on dispersed **21** powders (Γ) as a function of C_{eq} provide its adsorption isotherm (Figure 4), where the amount of **21** added was kept at 10 mM throughout this experiment. The pigment particles in low concentration of FPEG (closed circles in Figure 4) were sedimented without centrifugation. The surface coverage is seen to increase with increasing concentration of C_{eq} until a saturation value of 2.0 μmol m^{-2} (Γ_M) is attained at slightly above the critical micelle concentration of FPEG (8 μM). The arrow in this figure indicates the cmc. Such a correlation has been expected since both the cmc and the C_{eq}, when saturation is reached, reflect the affinity of the hydrophobic moiety of the surfactant to a nonpolar environment.[16] The value of Γ_M gives an area per molecule of 83 $Å^2$ $molecule^{-1}$. The adsorption of nonionic poly(oxyethylene)-type surfactants on a hydrophobic surface has been studied by a number of researchers.[16-20] In these studies, the values for $C_8\phi E_{9-10}$, $C_9\phi E_{10}$,

(16) Kronberg, B.; Kall, L.; Stenius, P. *J. Dispersion Sci. Technol.* **1981**, *2*, 215–232.
(17) Furlong, D. N.; Aston, J. R. *Colloids Surf.* **1982**, *4*, 121–129.

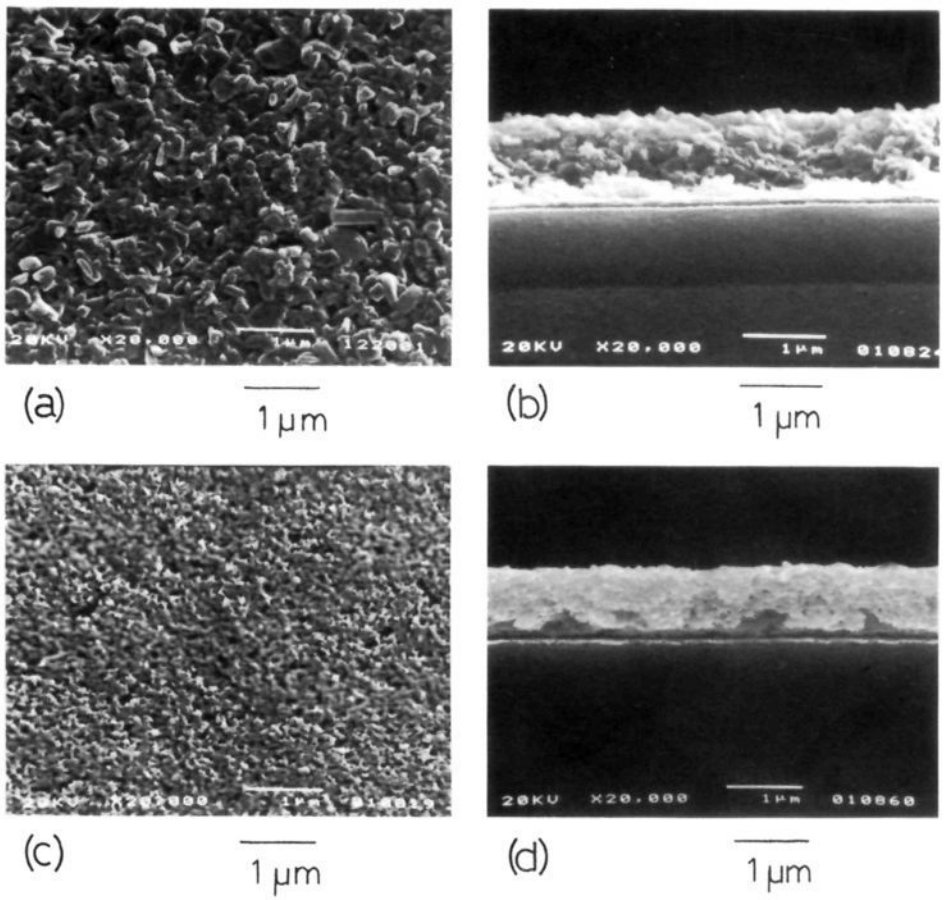

Figure 3. Scanning electron micrographs of surfaces and cross sections of the films prepared by the electrolysis of an aqueous solution containing **30** or **32**, 2.0 mM FPEG, and 0.1 M LiBr at the ITO electrode for 30 min: (a, b) **30**; (c, d) **32**.

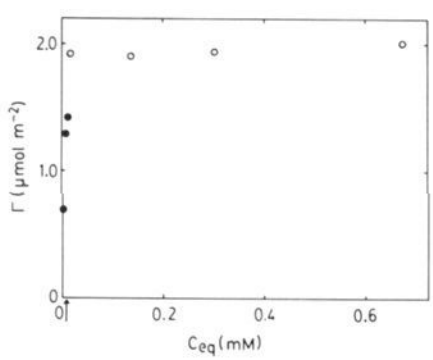

Figure 4. Adsorption isotherm of FPEG on **21** particles (10 mM). Closed circles indicate that **21** particles were sedimented without centrifugation. The arrow indicates the cmc of FPEG.

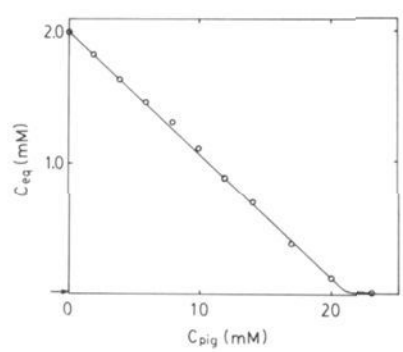

Figure 5. Equilibrium concentration of FPEG (C_{eq}) versus the amount of **21** particles (C_{pig}). Total concentration of FPEG was kept at 2.0 mM throughout the experiment.

$C_9\phi E_{15}$, and $C_8\phi E_{16}$ are 54, 54, 80, 131 Å^2 molecule^{-1}, respectively, where C, ϕ, and E stand for the hydrocarbon, phenyl, and ethylene oxide moieties, respectively, with subindices giving the length.[16,18,20] This agreement provides evidence for monolayer adsorption at saturation. The value of C_{eq} decreases linearly with increasing amount of **21** particles added (C_{pig}) (Figure 5). The inclination of the straight line in this figure gives the same value of Γ_M as that obtained by the adsorption isotherms. The pigment particles were sedimented at 27 mM of C_{pig}, which indicates that their sedimentation occurs by the desorption of 20% of the surfactant of the surface coverage.

On the basis of these results, we speculate the mechanism of the film formation through mechanism B of Scheme I as follows:

(i) The free surfactant (FPEG) diffuses to the electrode surface and is oxidized to its cation ($FPEG^+$). The concentration of free surfactant in the vicinity of the electrode decreases to less than the cmc.

(ii) The surfactants adsorbed on the pigment are desorbed from the pigment surface in order to satisfy the adsorption equilibrium. This desorption leads to the deposition of the pigment on the electrode, which occurs efficiently when the concentration of free surfactant decreases to less than the cmc.

(iii) After the electrode is covered with the pigment film, free surfactant diffuses in the film, owing to the existence of small space among the particles in the film, eventually reaches the electrode

(18) Kronberg, B.; Stenius, P.; Thorssell, Y. *Colloids Surf.* **1984**, *12*, 113–123.
(19) Partyka, S.; Zaini, S.; Lindheimer, M.; Brun, B. *Colloids Surf.* **1984**, *12*, 255–270.
(20) Boomgaard, T. V. D.; Tadros, T. F.; Lyklema, J. *J. Colloid Interface Sci.* **1987**, *116*, 8–16.

surface, and is electrolyzed. The concentration of free surfactant in the vicinity of the film is kept at less than the cmc so that the film continues to grow for a long period to respectable thicknesses.

Present experiments show that such an electrochemical method serves as a technique for preparing thin films of a wide variety of organic compounds. This technique may enable thin films of organic compounds to be prepared that satisfy the following conditions: (i) the organic compounds are soluble in a micellar solution or dispersible in a surfactant solution and (ii) they are not electrolyzed at the potential for oxidation of the surfactant with a ferrocenyl moiety (+0.3 V vs SCE for FTMA and +0.5 V for FPEG). Another important advantage of this technique is the fact that the starting organic compounds do not undergo electrochemical reactions when their films are formed; hence, film-forming compounds are the same as the starting compounds. Generally, electrochemical film formation proceeds via electrochemical reactions of the starting compounds, and the components of the film-forming compounds are different from those of the starting compounds.

Acknowledgment. We thank R. Ohki for the electron micrograph data. This work was partially supported by a Grant-in-Aid for Scientific Research from the Ministry of Education, Science and Culture (Nos. 62790219, 01604540, and 02205046).

Cysteine Conformation and Sulfhydryl Interactions in Proteins and Viruses. 1. Correlation of the Raman S-H Band with Hydrogen Bonding and Intramolecular Geometry in Model Compounds†

Huimin Li and George J. Thomas, Jr.*

Contribution from the Division of Cell Biology and Biophysics, School of Basic Life Sciences, University of Missouri—Kansas City, Kansas City, Missouri 64110. *Received April 19, 1990*

Abstract: The cysteine sulfhydryl group plays an important role in structural biochemistry. Cysteine thiols of proteins are capable of donating and accepting hydrogen bonds with solvent molecules as well as with other protein groups, and cysteine ligand coordination is fundamental to enzyme activity and nucleic acid recognition. We have undertaken a systematic Raman study of model mercaptans and cysteine thiols to provide an effective spectroscopic probe of the S-H group and its biologically relevant configurations and interactions in aqueous and crystalline proteins. The present study of aliphatic and aromatic mercaptans in both polar and apolar solvents, and of L-cysteine and glutathione in the crystal, provides a basis for interpreting the S-H stretching region of the Raman spectrum in terms of hydrogen bond donation by S-H, hydrogen bond acceptance by S, and rotamer populations of the cysteinyl side chain. The most definitive change observed in the Raman S-H stretching band is its shift to lower frequency when S-H acts as a hydrogen bond donor. We find further that the frequency interval in which the Raman S-H stretching vibration (σ_{SH}) occurs is diagnostic of S-H donors which are strongly hydrogen bonded (2525-2560 cm^{-1}), moderately hydrogen bonded (2560-2575 cm^{-1}), or weakly hydrogen bonded (2575-2580 cm^{-1}). When the S-H group is essentially non-hydrogen-bonded, e.g., at high dilution in CCl_4, we find $\sigma_{SH} \approx 2585 \pm 5$ cm^{-1}. On the other hand, hydrogen bond acceptance by S in the absence of S-H donation elevates σ_{SH} slightly (<4 cm^{-1}). In model mercaptans, P_C and P_H rotamers with respect to the C-C-S-H torsion (χ^2) yield σ_{SH} values that are separated by approximately 10 cm^{-1}, with the P_H rotamer generally exhibiting the higher frequency of the two. Since the S-H region of the Raman spectrum contains no interference from other molecular vibrations, the approximate 10-cm^{-1} shift should be measurable in proteins and thus should provide a means of resolving different cysteine side-chain orientations.

Introduction

Cysteine residues in proteins are capable of a variety of enthalpically favorable polar interactions which presumably contribute to the stabilization of the native structures. Hydrogen bonds involving the sulfhydryl group as donor (S-H···O) or the sulfur atom as acceptor (S···H-N) have been identified from both neutron and X-ray diffraction studies of model compounds (reviewed in ref 1-3). Similar donor-to-acceptor distances determined in protein crystallographic analyses are consistent with sulfhydryl hydrogen bonding in proteins.[4,5] Polar interactions of cysteinyl S and S-H groups with protein aromatic side chains have also been proposed.[6] A common feature of such interactions is the requirement of a shift of electron density from the donor hydrogen toward its covalently bonded sulfur, yielding $^{\delta-}S-H^{\delta+}$ partial charge separation, thereby facilitating favorable interaction at either end of the dipole with an appropriate, oppositely charged group. Thus, a sulfhydryl group that participates in hydrogen bonding or aromatic interaction is expected to exhibit S-H covalency somewhat altered from that of an isolated or noninteracting S-H group. At present, little is known about the energetics of such bonding in proteins and the possible contributing effects of solvent and neighboring protein groups.

The sulfhydryl group of cysteine is also one of the most chemically reactive functional groups in a protein,[7] confirming its nucleophilic nature and the polarity of the sulfhydryl bond. The wide use of sulfhydryl reagents as probes of protein structure and cysteine accessibility underscores the need for additional structural information about interacting S-H groups in proteins, particularly those of aqueous proteins and their assemblies.

† This is paper 32 in the series, Studies of Virus Structure by Raman Spectroscopy. Supported by NIH Grant A111855.

* To whom correspondence should be addressed.

(1) Taylor, R.; Kennard, O. *J. Am. Chem. Soc.* **1982**, *104*, 5063-5070.
(2) Taylor, R.; Kennard, O. *Acc. Chem. Res.* **1984**, *17*, 320-326.
(3) Burley, S. K.; Petsko, G. A. *Adv. Protein Chem.* **1988**, *39*, 125-189.
(4) Birktoft, J. J.; Blow, D. M. *J. Mol. Biol.* **1972**, *68*, 187-240.
(5) Wilkinson, A. J.; Fersht, A. R.; Blow, D. M.; Winter, G. *Biochemistry* **1983**, *22*, 3581-3586.
(6) Reid, K. S. C.; Lindley, P. F.; Thornton, J. M. *FEBS Lett.* **1985**, *190*, 209-213.
(7) Lundblad, R. L.; Noyes, C. M. *Chemical Reagents for Protein Modification*; CRC Press: Boca Raton, FL, 1984; Vol. I, pp 55-93.

0002-7863/91/1513-456$02.50/0